Accepted Manuscript

Specific profile of Tempranillo grapevines related to Esca-leaf symptoms and climate conditions

Laura Martín, Florence Fontaine, Francisco Javier Castaño, Aurelie Songy, Rafael Roda, Julie Vallet, Raúl Ferrer-Gallego

PII: S0981-9428(18)30487-X

DOI: https://doi.org/10.1016/j.plaphy.2018.10.040

Reference: PLAPHY 5482

To appear in: *Plant Physiology and Biochemistry*

Received Date: 19 April 2018

Revised Date: 23 October 2018

Accepted Date: 31 October 2018

Please cite this article as: L. Martín, F. Fontaine, F.J. Castaño, A. Songy, R. Roda, J. Vallet, Raú. Ferrer-Gallego, Specific profile of Tempranillo grapevines related to Esca-leaf symptoms and climate conditions, *Plant Physiology et Biochemistry* (2018), doi: https://doi.org/10.1016/j.plaphy.2018.10.040.

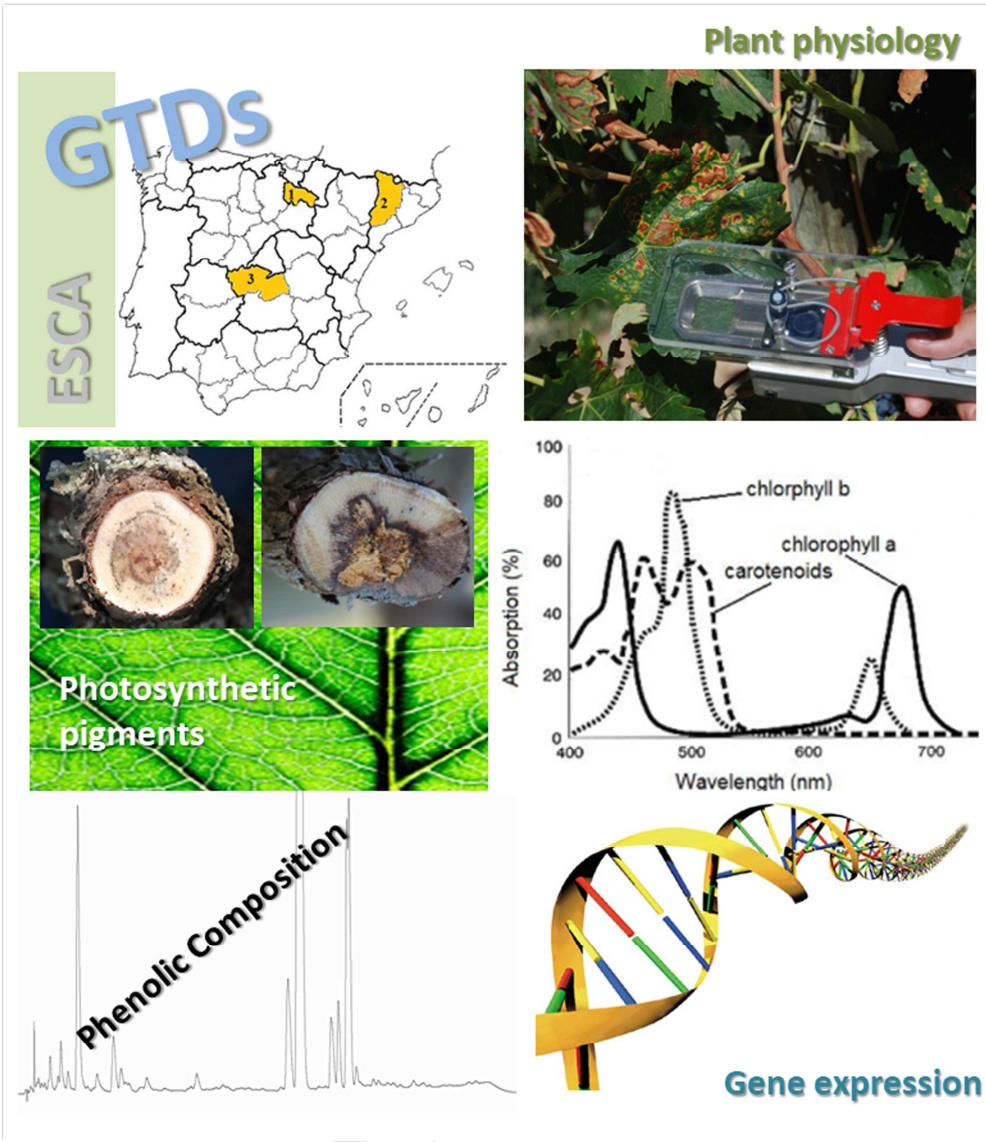
Plant physiology
GTDs
ESCA
1
2
3
Photosynthetic pigments
chlorphyll b
chlorophyll a
carotenoids
Absorption (%)
Wavelength (nm)
Phenolic Composition
Gene expression

Title

Specific profile of Tempranillo grapevines related to Esca-leaf symptoms and climate conditions.

Authors

Laura Martín[1,3*], Florence Fontaine[2], Francisco Javier Castaño[1], Aurelie Songy[2], Rafael Roda[1], Julie Vallet[2] and Raúl Ferrer-Gallego[1].

[1] Wine Technology Centre (VITEC), Ctra. de Porrera km 1, 43730 Falset, Tarragona (Spain).

[2] SFR Condorcet, FR CNRS 3417, Université de Reims Champagne-Ardenne, URVVC EA 4707, Résistance Induite et Bioprotection des Plantes, BP 1039, Reims, Cedex 2 51687, (France).

[3] Centro de Investigaciones Científicas y Tecnológicas de Extremadura (CICYTEX) Department of Phytopathology. Instituto de Investigaciones Agrarias Finca La Orden-Valdesequera. Autovía A-5, km 372 - 06187 Guadajira, Badajoz (Spain)

*Corresponding author: laura.martin@juntaex.es

Abstract

Esca is a destructive fungal disease affecting grapevines worldwide. In the Esca complex, grapevine leaf stripe disease (GLSD) designates specifically the disease that causes the typical leaf symptoms on infected vines. Understanding foliage alterations produced by GLSD may help to identify potential markers of tolerance to this disease. In this work, changes related to physiological parameters, photosynthetic pigments and phenolic compounds were evaluated. Moreover, the expression of 10 genes was tracked determined by quantitative reverse transcription-PCR. For this, symptomatic and asymptomatic vines from three different Tempranillo vineyards were evaluated. Vineyards differed in climate classification and water resources. Botryosphaeriaceae species and Esca causal agents (*Phaeomoniella chlamydospora*, *Phaeoacremonium* spp. and *Fomitiporia mediterranea*) were isolated and identified from symptomatic vines. Under water restriction, a significant decrease on the physiological activity of symptomatic vines was observed. Also, symptomatic leaves showed lower content on chlorophylls and carotenoids and some alterations on their phenolic profiles. GLSD symptoms induced the expression of defense-related genes, especially *PR6*, *STS* and *Chit 1b*. This research provides valuable information regarding physiological, chemical and molecular changes in Esca affected leaves of Tempranillo grown in vineyards related to the climate conditions.

Keywords

Defense response, Esca, GLSD, irrigation, phenolic compounds, photosynthesis, vineyard.

1. INTRODUCTION

Grapevine trunk diseases (GTDs) decrease both quality and yield of grapevines (*Vitis vinifera* L.) all over the world. The worldwide annual cost due to GTDs was estimated to be about 1.1€ billion euros (for review see De la Fuente et al., 2016). Currently, no curative treatment is available to reduce the impact of GTDs in both newly established and adult vineyards (Gramaje et al., 2018; Mondello et al., 2018). In established vineyards, Esca complex is the most destructive of GTDs, especially in Europe, being a major concern on viticulture because of the rapid and dramatic increase of its incidence (Bertsch et al., 2013; De la Fuente et al., 2016). Consequently, numerous studies have been conducted to assess the etiology of GTDs (for review Bertsch et al., 2013 and Gramaje et al., 2018). Esca disease is present in all vine-growing regions affecting diverse varieties. Tempranillo, the most widespread cultivar in Spain (201.051 Ha in 2015) with an important cultivation also in South America and Portugal (synonym "Aragonez"), is known as susceptible to GTDs (Luque et al., 2009; Martín and Martín, 2013; De la Fuente et al., 2016).

Esca is a complex disease comprising several syndromes among which 'grapevine leaf stripe disease' (GLSD) and Esca proper (commonly refers to white rot caused by the basidiomycete *Fomitiporia mediterranea*) are prevalent in European vineyards. Typical external foliar symptoms of the Esca complex are either yellow-brown or red–brown interveinal areas, resulting in a "tiger-striped" pattern (Mugnai et al., 1999). The term GLSD was proposed to designate specifically the disease that causes the typical leaf symptoms on infected grapevines (Surico, 2009). Some of the plants affected by GLSD do not show symptoms every year (Bertsch et al., 2013; Calzarano et al., 2017b; Mondello et al., 2018), making it difficult to externally distinguish infected and non-infected plants. Severe Esca, named "apoplexy", is characterized by a rapid basipetal

wilt of entire vines, including the grape clusters (Mugnai et al., 1999). Internal symptoms of Esca disease include dark streaking of the xylem tissues and white rot (Larignon and Dubos, 1997; Mugnai et al., 1999; Bertsch et al., 2013). A classical diagnosis of Esca complex is completed by performing an invasive and destructive analysis of the wood in order to isolate the causal agents. The main causal agents of GLSD are considered to be the tracheomycotic agents *Phaeomoniella chlamydospora* (Chaetothyriales, Herpotrichiellaceae) (Crous and Gams, 2000; Larignon and Dubos, 1997; Bertsch et al., 2013;); and multiple *Phaeoacremonium* species (Diaporthales, Togniniaceae) (Larignon and Dubos, 1997; Martín and Martín, 2013; Bertsch et al., 2013; Gramaje et al., 2015). White wood rot is caused by several basidiomycetes species, among which the most common in Europe is *Fomitiporia mediterranea* (Fischer, 2002; Bertsch et al., 2013; Fischer and González García, 2015). All these pathogens are localized in the woody tissues of perennial organs but never in leaves, where symptoms are expressed. Their isolation and identification from wood are time consuming and not practical for the diagnosis and monitoring of Esca emergence in vineyards. Until now, the visual observation in the field of both foliar GLSD and berry symptoms is the only non-disruptive way to identify it. The complexity of Esca disease epidemiology, i.e. many pathogens involved, inconstancy and latency time to the appearance of external foliar symptoms, makes difficult the diagnosis, the management, and the research on Esca control strategies (Calzarano et al., 2014; Gramaje et al., 2018; Mondello et al., 2018).

Studying the changes occurring in leaves and prior to any visible outbreak as a response to Esca pathogens infection may help in this concern. In grapevines, the response of leaves to fungal pathogen attacks such as *Botrytis cinerea* or *Plasmopara viticola* is relatively well-documented especially in terms of i) changes in carbohydrate

metabolism through the perturbation of photosynthesis or gas exchange (Moriondo, 2005), ii) triggering of defense responses (Kortekamp, 2006; Chong et al., 2008), and iii) modifications on the phenolic profile including phytoalexins production (Hasan and Bae, 2017). For the relationships between Esca pathogens and grapevine physiology, only few researches are conducted. To date, studies on these effects have been carried out using *in vitro*-grown plants or calluses artificially infected with only one pathogenic fungus species (Bruno and Sparapano, 2006; Martin et al., 2009). Little is still known on the physiological impact of Esca on plants grown in vineyards that are usually infected by several Esca pathogens. Some studies concerning white cultivars, such as cv. Alvarinho (Lima et al., 2017), cv. Chardonnay (Petit et al., 2006; Magnin-Robert et al., 2011, 2017;) and cv. Ugni Blanc (Valtaud et al., 2011), reported physiological alterations produced by Esca in leaf samples. Altogether, these changes involve a decline of the photosynthetic rate affecting the carbohydrate metabolism. An induction of defense mechanisms, especially the glutathione pathway, PR-proteins such as β-1,3-glucanases or chitinases, as well as an accumulation or alteration of phenolic compounds like stilbenes, hydroxycinnamic acids and flavonols have been described in various white cultivars such as Chardonnay, Ugni blanc, Alvarinho and Trebbiano d'Abruzzo (Fontaine et al., 2016; Calzarano et al., 2016, 2017a). In addition, both Esca susceptibility and defense response have been shown to differ among cultivars (Martin et al., 2009; Lambert et al., 2013). The knowledge related to the impact of Esca - GLSD on the physiology of red cultivars is scarce (Lambert et al., 2013) and has not been yet studied in cv. Tempranillo under field condition.

The main objective of this work was to elucidate the Tempranillo response, a red cultivar, to Esca - GLSD in grown vineyards at physiological, molecular and chemical level. To achieve this goal, three different Spanish geographical regions with dissimilar

115 climate conditions and irrigation availability were considered. Seven physiological
116 parameters of leaves with GLSD symptoms were compared with those of asymptomatic
117 leaves. The infection of the wood was checked by isolation and identification of GTD
118 pathogens. Results confirmed infection in symptomatic vines and no infection by GTD
119 in asymptomatic ones. Changes on the photosynthetic pigments and the phenolic
120 composition of symptomatic and asymptomatic leaves were evaluated. Moreover, the
121 expression of ten genes involved in defense response and physiology was investigated.
122

123 ## 2. MATERIALS AND METHODS

124 ### 2.1. Plant material

125 Experiments were performed on leaves of cv. Tempranillo grown in commercial
126 vineyards. Three different geographical Spanish regions were considered. Vineyard 1
127 was located in Rioja region (Figure 1a) with an average annual temperature of 12.7 °C
128 registered during the four years (2013-2016) of the study (average of maximum
129 temperatures in the warmest month, July 29.7 ºC, and average of minimum
130 temperatures in the coldest month, February 1.98 ºC). The cumulative average (2013-
131 2016) precipitation was 523.38 mm (Table 1). The Köppen-Geiger climate classification
132 is Csb (warm temperature climate with a dry and warm summer) (Kottek et al., 2006).
133 This vineyard was planted in 1994 (19 years old in 2013) with a planting arrangement
134 of 2.2 m x 1 m, grafted on 110-R rootstock and trained according to the vessel system
135 under drought (without irrigation). Vineyard 2 was located in Catalonia region (Lleida)
136 with an average (2013-2016) annual temperature of 14.1 °C (average of maximum
137 temperatures in the warmest month, July 36.4 ºC, and average of minimum
138 temperatures in the coldest month, December -4.6 ºC), and 357.68 mm of cumulative
139 annual (average 2013-2016) precipitation (Table 1). The Köppen-Geiger climate

140 classification is Cfa (warm temperature climate; fully humid with a hot summer)
141 (Kottek et al., 2006). This vineyard was planted in 1997 (16 years old in 2013) with a
142 planting arrangement of 3 m x 2 m, grafted on 110-R and trained on a bilateral cordon
143 with sprinkler irrigation. Vineyard 3 is located in Castilla La Mancha region (Toledo)
144 with an average (2013-2017) annual temperature of 15.5 °C (average of maximum
145 temperatures in the warmest month, July 35.4 ºC, and average of minimum
146 temperatures in the coldest month, January -0.22 ºC), and 319.54 mm of cumulative
147 annual (average 2013-2017) precipitation (Table 1). The Köppen-Geiger climate
148 classification is Csa (warm temperature climate with a dry and hot summer) (Kottek et
149 al., 2006). This vineyard was planted in 2002 (11 years in 2013) with a planting
150 arrangement of 3 m x 1.5 m, grafted on 110-R and trained on a bilateral cordon with
151 drip irrigation.
152 Foliar Esca symptoms of 600 Tempranillo vines subdivided in 200 each per vineyard
153 were visually monitored since 2013. During the time of the experimentation, GLSD
154 incidence was 6.3% to 11.4 % in Vineyard 1; 29.6 % to 30.0 % in Vineyard 2; and 1.2%
155 to 3.0% in Vineyard 3. Visually, two groups of plants were identified in each
156 geographical region: (i) vines showing no GLSD symptoms (namely *Asymptomatic, A*);
157 and (ii) vines that developed GLSD symptoms that were considered as diseased plants
158 (namely *Symptomatic, S*). Only vines without any foliar symptoms during the four
159 monitoring years were considered as asymptomatic (A). The wood analysis (see section
160 2.2 below) resulted in no isolation of GTD fungi from A vines and confirm infection of
161 S vines.
162 Leaf symptomatic plants infected by Esca (GLSD) showing large necrotic areas do not
163 allow correct physiological measurements with the gas analyzer (Di Gennaro et al.,
164 2016). Moreover, RNA from leaves with severe Esca symptoms could not be properly

analyzed because of its low abundance and poor quality by Valtaud et al. (2011). To avoid such inconveniences in this research leaves' collection and measurements were performed at the beginning of the appearance of the first foliar symptoms (Figure 1b). Based on the field evaluation of GLSD and the results of wood analysis, four different vines for each condition (A and S) and vineyard (from 1 to 3) were selected. On the selected vines: i) the physiological activity was measured in two consecutive years and ii) at the same time, three leaves per plant were collected, immediately frozen (*in situ*) in liquid nitrogen and stored at -80 ºC until the molecular and chemical analyses were performed.

2.2. Isolation and identification of pathogens in wood samples

To assess the fungal infection of all S and A grapevines, cross and longitudinal sections of the woody stem (part of an arm or cordon > 5 years old) were brought to the laboratory and analyzed. Samples were collected at pruning time after the first year of visual evaluation. The causal agents of Esca were isolated throughout culturing six small wood pieces per section in rich medium (malt extract agar amended with 0.25 mg/mL chloramphenicol). The observed fungi were transferred individually to fresh medium, and pure colonies were obtained to conduct a morphological and molecular identification. For molecular identification, the total genomic DNA was isolated and amplified from fresh mycelium using the REDExtract-N-Amp Kit (XNAP) (Sigma, St. Louis, Missouri, USA) following manufacturer's instructions. The internal transcribed spacer (ITS) region ITS1-5.8S-ITS2 (primers ITS4 and ITS5; White et al., 1990) was amplified in all isolates used for phylogenetic analysis. Identification of *Fomitiporia mediterranea* and *Phaeomoniella chlamydospora* was confirmed by sequencing analysis of the ITS, while for the identification of *Phaeoacremonium* species, analysis

of the β-tubulin (BT) gene, amplified with primers T1 (O'Donnell and Cigelinik, 1997) and Bt2b (Glass and Donaldson, 1995) were needed. The PCR amplification was performed using the XNAP Kit following the protocols and conditions previously reported (Martín and Martín, 2013). The sequences were then read and edited using Chromas v.1.45 software and consensus sequences were compared with those available in the GenBank database by using the Basic Local Alignment Search Tool (BLAST) in order to identify homologous sequences. Fungal isolates morphologically identified as members of the Botryosphaeriaceae family were confirmed by using the Qualiplante SAS End-Point Botryosphaeria Nested PCR kit (Qualiplante, Clapiers, France) following supplier's conditions. The oligonucleotide primer set DS3.8S3-DS3.8R6 was used to rapidly identify *Diplodia seriata* isolates (Martín et al., 2014). All PCR amplifications were performed using a T100^{TM} thermal cycler (BioRad). Primer sets were supplied by Biomers (Söflinger, Germany) and sequences were obtained using the Macrogen DNA sequencing services (South Korea).

A phylogenetic analysis was performed using the ITS dataset. The analysis involved 30 nucleotide sequences: 16 from fungi isolated in this work aligned with 14 further sequences from GenBank. All positions containing gaps and missing data were eliminated. There were a total of 459 positions in the final dataset. The evolutionary history of the aligned ITS data was inferred using the Neighbor-Joining (NJ) method, employing MEGA v.6.0 software (Tamura et al., 2013). The robustness of the internal branches (percentage in which the associated taxa clustered together) was evaluated by 1,000 bootstrap replications. Sequences divergence were computed using the Kimura 2-parameter method (Kimura, 1980). The NJ tree (Figure 2) is drawn to scale according to the number of base substitutions per site and graphically represents the evolutionary distances.

2.3. Physiological measurements

Following visual characterization and wood analysis, the changes in physiological activity were followed-up during the next two consecutive years. It was in 2015 and 2016 for vineyards 1 and 2. In the vineyard 3, the study was completed during 2016 and 2017. Measurements of leaf water potential (Ψ_{leaf}) and gas exchange were performed on asymptomatic (A) and symptomatic (S) leaves when first foliar symptoms appeared. Phenological stage was beginning of berry ripening (81 according to BBCH scale) in all cases. During the first year, it was on July 7th, on June 19th and on August 3rd, for vineyards 1, 2 and 3 respectively. During the second year, it was on July 19th, on July 12th and on July 26th (Table 3). Physiological determinations were performed on two leaves per vine from four different plants of each of the two groups of vines. Results are presented as mean ± standard errors of eight repetitions (n = 8) per condition, i.e. A and S. The plant water status was estimated by the Ψ_{leaf} parameter and measured with a Scholander chamber (Soil Moisture Equipment Corp., USA). Leaf temperature, net leaf photosynthesis (A_N), stomatal conductance (gs), transpiration (E) rates and the internal leaf CO_2 concentration (C_i) were determined simultaneously on leaves with a portable infrared gas analysis system (IRGA) (LCI Portable Photosynthesis System, ADC BioScientific Ltd, Hoddesdon, England). The intrinsic water use efficiency (WUEi) was determined by the ratio of A_N/gs that provides the cost of water for the CO_2 assimilation (Tomás et al., 2014). The IRGA was equipped with a clamp-on leaf cuvette that exposed 6.25 cm^2 of leaf area and PAR (Photosynthetic Active Radiation) was always above saturation level. All measurements were done in sun exposed and adult leaves located in the middle part of the cane and performed from 9.00 to 11.00 a.m., just before midday depression, according to other authors (Cartechini and Palliotti, 1995).

2.4. Photosynthetic pigments

To quantify photosynthetic pigments, three leaves per plant were collected on the same four vines per condition (A and S) and vineyard (from 1 to 3) used for physiological determinations. The analysis was achieved on the leaves collected in 2016 for all three vineyards. Collection dates are detailed in section 2.3 and Table 3. Determinations were repeated three times. Results are presented as mean ± standard errors of twelve repetitions (n = 12) per condition. Chlorophyll and carotenoid contents were extracted from freeze dried leaves (50 – 60 mg) in the dark in 10 mL of acetone:water (80:20) during 15 min in ultrasonic bath. The extraction was performed twice and the obtained extracts (25 mL) were filtered (0.45 µm pore size) and measured as following. The chlorophylls (Chl *a* and Chl *b*) and carotenoids (C_{c+x}) were analysed by UV-VIS spectroscopy using a Helios Alpha (ThermoFisher, USA) spectrophotometer in 1 cm plastic cuvettes. The concentrations were calculated by the equations (1-3):

(1) Chl $a = 12.25A_{663nm} - 279A_{645nm}$

(2) Chl $b = 21.5A_{645nm} - 5.1A_{663nm}$

(3) $C_{x+c} = (1000A_{470nm} - 1.82\text{Chl } a - 85.02\text{Chl } b)/198$

2.5. Phenolic extraction and HPLC-DAD-MS analysis

To characterize the phenolic composition, three leaves per plant were collected on the same four vines per condition (A and S) and vineyard (from 1 to 3) used for physiological determinations. The analysis was achieved on the leaves collected in 2016 for all three vineyards. Collection dates are detailed in section 2.3 and Table 3. Determinations were repeated twice. Results are presented as mean ± standard errors of eight repetitions (n = 8) per condition. Freeze dried leaf samples (1.0 – 2.0 g) were homogenized and extracted in the dark with 10 mL of methanol during 48 h of stirring. The liquid phase was centrifuged for 5 min (6000 r.p.m.) and the supernatant was

collected and concentrated under vacuum by a SavantTM SPD121P SpeedVac™ and redisolved in 1 mL of methanol. The liquid phase was filtered (0.45 µm) and 100 µL of sample were injected into the chromatographic system. Chromatographic analysis was performed using an Agilent 1200 Series HPLC system consisting of a degasser, ALS, Quat Pump, DAD + FLD, controlled by ChemStation software (version B.04.01; Agilent Technologies, Waldbronn, Germany). A Zorbax Eclipse Plus 4.6 mm x 150 mm, 5 µm column thermostatted at 35 ºC was used. The mobile phase was (A): aqueous solution of trifluoroacetic acid (0.1%) and (B): acetonitrile HPLC-grade. The isocratic gradient used was 10% B for 5 min, from 10 to 15% B for 15 min, isocratic 15% B for 5 min, from 15 to 18% B for 5 min and from 18 to 35% B for 20 min, at a flow rate of 0.5 mL/min. Spectra were recorded from 220 to 600 nm. Double online detection was carried out in the DAD using 360 nm as preferred wavelength and in a mass spectrometer (MS) connected to the HPLC system via the DAD cell outlet. MS detection was performed in a TSQ Quantum™ Access MAX (ThermoFisher Scientific) equipped with an HESI source which was operated in the negative ionization mode between *m/z* 100 and 1000. The HESI spray voltage was set at 3.5 kV and the capillary temperature was maintained at 360 °C. Nitrogen was used as the sheath gas (60 arb.) and auxiliary gas (20 arb.) for nebulization and desolvation. The vaporizer temperature was maintained at 350 °C. Argon was used as the collision gas for collision-induced dissociation.

2.6. RNA extraction, quantitative Reverse Transcription–PCR (qRT-PCR) and analysis of gene expression

To study defense responses, three leaves per plant were collected on the same four vines per condition (A and S) and vineyard (from 1 to 3) used for physiological determinations. The analysis was performed on leaves collected in 2015 for vineyards 1

and 2; and the leaves collected in the last year (2017) for vineyard 3. Collection dates are detailed in section 2.3 and Table 3. Total RNA was isolated from 50 mg of ground powder using a plant RNA Purification Reagent Kit (Invitrogen, Cergy Pontoise, France), re-suspended in 20 µL of RNase-free water, and treated with RQ1 DNase enzyme (Promega, Madison, W1, USA). After that the RNA was quantified by measuring the absorbance at 260 nm. A Verso cDNA synthesis kit (Thermo Scientific) was used for reverse transcription of 150 ng of total RNA. The expression of two photosynthesis-related genes (*RbcL* and *SBP*), of the *PIP 2.2* intrinsic aquaporin, of two genes involved on the detoxification process (*EpoxHF* and *SOD*) and of six defense-related genes were determined by qRT-PCR using the primers indicated in Table 2. The reactions were carried out in a real-time PCR detector Chromo 4 apparatus (Bio-Rad, Hercules, CA, USA) using the thermal profile previously described (Magnin-Robert et al., 2011). For each experiment, PCR reactions were performed in duplicate and two independent experiments were analyzed. The relative levels of gene expression were determined, following the methods of Hellemans et al. (2007), with the EF1- α and 60SRP genes as internal reference genes. Results represent the relative expression of genes in leaves from S plants versus leaves collected from A plants. Gene expression was considered as significantly up- or down-regulated relative to the 1X controls when changes in relative expression were >2X or <0.5X, respectively.

2.7. Statistical analysis

A simple analysis of variance (ANOVA) was carried out to determine significant differences between S and A samples using the StatGraphics Centurion XVI (Manugistics Inc., Pockville, MD, USA) program. The Tukey's procedure was used for discriminating among the means of the variables. Differences at $p < 0.05$ were considered significant.

3. RESULTS AND DISCUSSION

3.1. Isolation and identification of pathogens in vine wood samples

No pathogen was detected in the healthy wood of asymptomatic (A) grapevines used in this work. As a result, A vines might be asymptomatic or healthy vines. In symptomatic (S) grapevines, cross and longitudinal sections of the wood showed different types of necrosis including white rot (view images in the graphical abstract). From the symptomatic wood of S plants the phytopathogenic species *Phaeomoniella chlamydospora* and *Fomitiporia mediterranea* as well as members of the Botryosphaeriaceae family and *Phaeoacremonium* spp. were isolated (Table S1). In this work, the Qualiplante SAS End Point Botryosphaeria nested PCR kit allowed the amplification of isolates morphologically identified as Botryosphaeriaceae. However, there was no difference among *Diplodia seriata* and *Neofusicoccum parvum* amplicons. A total of 12 species belonging the Botryosphaeriaceae family and mostly related to GTDs was previously detected using this methodology (Martín et al., 2015). The oligonucleotide primer set DS3.8S3-DS3.8R6 specifically confirmed *D. seriata* in 9 out of the 12 S vines. Sixteen isolates were selected to represent a molecular phylogenetic analysis of the ITS region and the obtained tree is shown in Figure 2. The specie *N. parvum* was identified from vineyard 1 when analyzing the sequences of the ITS region, but it did not amplify using the primer set DS3.8S3-DS3.8R6. For *Phaeoacremonium* spp., the partial sequencing of the β-tubulin gene confirmed the identification of *Pm. minimum, Pm. iranianum and Pm. viticola* showing 99-100% similarity to corresponding sequences deposited under JF275878, JF275873, and HQ700718 (Martín and Martín, 2013), respectively. In the present study, the GLSD causal agents (*Phaeoacremonium minimum, Pm. iranianum* and *Pm. viticola* and *P. chlamydospora*)

as well as *F. mediterranea* related to "Esca proper" (Bertsch et al., 2013; Calzarano et al., 2014; Fontaine et al., 2016) were confirmed to infect the wood of symptomatic grapevines.

Differences in fungal species were found depending on geographical regions and climate conditions. *Diplodia seriata* and *Pm. minimum* were isolated in the three studied vineyards. The predominantly isolated pathogens in both vineyards 1 and 2 belonged to Botryosphaeriaceae family (mostly *D. seriata*). Botryosphaeriaceae and Hipocreaceae have been found to be the most abundant fungi colonizing the healthy wood tissues of Esca symptomatic or asymptomatic plants (Bruez et al., 2014). *Phaeoacremonium minimum* was the main pathogen found in vineyard 3, confirming this taxon as one of the main causal organisms in GLSD diseased young vines (Martín and Martín, 2013; Gramaje et al., 2015). Simultaneous co-infections in the branch of one S plant by two or more pathogens were recurrent, with *Pm. minimum* plus *D. seriata* being the most common combination (Table S1).

3.2. Vine physiological parameters

We studied the physiological response to Esca disease in Tempranillo grown vineyards in three different geographical areas under various climate conditions (Table 3). As expected, grapevines differed in their water status and physiology behavior conferring to the geographical region and climate classification. According to other authors (Hidalgo and Hidalgo, 2011) and based on the leaf water potential (Ψ_{leaf}), no water restriction was observed for the leaves from vineyards 1 and 2 (values ranged from -0.72 to -0.91MPa) during the two studied years (2015 and 2016). However, severe (from -1.45 to -1.48 MPa) and medium (from -1.12 to -1.27 MPa) restriction of water was found in leaves from the vineyard 3 for the first (2016) and the second year (2017), respectively (Hidalgo and Hidalgo, 2011). In general, symptomatic leaves (S) showed

higher Ψ_{leaf} (-0.91; -0.72; -0.87 -0.90; -1.48; - 1.27 MPa) than asymptomatic (A) (-0.81; -0.87; -0.82; -0.81; -1.45; -1.12 MPa), although no significant differences were observed. Data sorted by the first and second year in vineyard 1, vineyard 2 and vineyard 3, respectively (Table 3). At times, the temperature of S leaves was also greater (35.08; 35.83; 36.67 ºC) than the temperature of A leaves (34.20; 35.46; 35.85 ºC), as occurred for vineyard 1 (in 2015 and 2016) and vineyard 2 in 2016 (complete data in Table 3). These results suggest that fungal infection did not directly disturb the plant water status in the leaf at early appearance of symptoms. Conversely, in Trebbiano d'Abruzzo cv. the water concentration on average was 65% in full symptomatic (tiger-striped) leaves, and 72% in both healthy and asymptomatic/diseased leaves (Calzarano et al., 2016). According to previous work (Escalona et al., 1999), vineyard 1 and 2 showed normal values in the others physiological parameters such as net leaf photosynthesis (A_N), stomatal conductance (gs) and transpiration (E). Results obtained in vineyard 3 during the first year (2016) showed significant differences between the two groups of vines with A_N, gs, and E values of 8.26 µmol/m2s, 0.09 mol/m2s, and 3.85 mmol/m2s for A vines and 4.83 µmol/m2s, 0.04 mol/m2s and 1.97 mmol/m2s for S vines, respectively. These results suggest that, in Tempranillo, GLSD symptomatic leaves suffer a significant decrease of A_N, gs and E under water stress conditions defined by Ψ_{leaf} < -1.4 MPa (Hidalgo and Hidalgo, 2011) and gs < 0.150 mol/m^2s (Escalona et al., 1999). In the meantime, a significant decrease of the internal leaf CO_2 concentration (Ci) was generally noted in S vines compared to the A vines, especially for vineyard 3 (126.0 and 160.7 µmol/m^2s, respectively). In the same year, the calculated intrinsic water use efficiency in vineyard 3 (WUEi) was also significantly higher in S vines (126.4 and 107.1) than in A vines (99.51 and 94.80). A similar pattern was observed in vineyard 2 despite the values were somewhat lower (54.2 and 69.2 for

S vines and 48.8 and 57.6 for A vines). In vineyard 1, the WUEi ratio was superior in A leaves (71.29 in 2015 and 76.14 in 2016) versus S vines (56.13 in 2015 and 73.25 in 2016). The obtained results suggest that in the leaves of S vines at early appearance of symptoms as the Ψ_{leaf} decreases, A_N and gs decrease too, whereas WUEi increases. Such observations are consistent with previous works that reported limitations of Tempranillo photosynthesis in water stressed field-grown vines (Escalona et al., 1999). A decrease of both A_N and gs was also observed in leaves of cv. Chardonnay (Petit et al., 2006) and was correlated with the chronology of the appearance of Esca symptoms (Magnin-Robert et al., 2011) and apoplexy (the severe and rapid form of Esca disease) (Letousey et al., 2010), but neither the water status nor the geographical or climate growing conditions were considered. In Tempranillo, GLSD symptomatic leaves with high values of WUEi and low concentrations of Ci were found opposing to that reported for Chardonnay (Petit et al., 2006; Letousey et al., 2010). Our results suggest that photosynthesis disturbance in the early stage of GLSD symptoms expression in Tempranillo leaves might be due in part to stomatal closure and it could be intensified under drought conditions.

3.3. Photosynthetic pigments

To determine the effect of GLSD on Tempranillo leaves, the content of chlorophylls and carotenoids were measured in 2016 when first foliar symptoms appeared. The range of values for both A and S vines differed among vineyards (Figure 3). The highest amount of chlorophylls was found in leaves of vineyard 1 (> 7 mg/g), while values around 5 and 3 mg/g were found in vineyards 2 and 3, respectively. Accordingly, vineyards with higher content of chlorophylls showed higher content of carotenoids. Vineyard 1 and 2 showed ≥ 1 mg/g of carotenoids whereas the vineyard 3 showed values around 0.75

mg/g. The lowest amount of both types of pigments was found in vineyard 3. Related to physiology (section 3.2 and Table 3), vineyard 3 showed a minor activity on gas exchange (A_N, gs and E) and a severe restriction of water at time of samples collection. Taking into account all these results, it seems that the total content of photosynthetic pigments is influenced by factors related to climate and/or geographical areas, as well as the water and physiological status of the grapevine.

Interestingly, all photosynthetic pigments were noticeably affected by GLSD. Significant differences between A and S leaves were observed in the investigated vineyards (Figure 3). Total chlorophylls (Chl *a* + Chl *b*) significantly decreased in S leaves from vineyards 1 and 3, and was analogous with A vines in vineyard 2 (Figure 3). Moreover, under all three vineyards conditions, the content of carotenoids registered in the A vines was significantly higher than those observed in S leaves. This study confirms that both total chlorophylls and carotenoids tend to decrease in GLSD symptomatic leaves of cv. Tempranillo at the early appearance of symptoms. Similar patterns were found on Esca infected plants of cvs. Chardonnay (Petit et al., 2006) and Ugni Blanc (Valtaud et al., 2011). Such results suggest that the decrease of photosynthetic activity (A_N) in GLSD affected vines is linked with the reduction of the photosynthetic pigments. In fact, the decrease in photosynthetic activity may be associated with a degradation of the photosynthetic pigments as reported in grapevines infected with phytoplasma (Bertamini et al., 2002).

3.4. Phenolic composition of Tempranillo leaves

In this study, a total of 23 phenolic compounds have been identified in Tempranillo leaf samples (Table 4 and Figure 4). Among the phenolic compounds identified, flavonols were the predominant flavonoids and hydroxycinnamic acids were the predominant non-flavonoids compounds. These compounds are abundant in grapevine leaves and

have been recently related to Esca disease, showing a significantly increase in diseased leaves of Alvarinho (Lima et al., 2017). Figure 4 shows differences in the phenolic composition of asymptomatic (A) and symptomatic (S) leaves in the three studied vineyards. Differences for each chromatogram peak number were observed between A and S, especially in vineyards 1 and 2. In vineyard 3, only slight modifications in the phenolic composition are apparent. For vineyards 1 and 2, twelve and eleven significant differences were found between A and S samples, respectively. The significant differences observed in vineyard 1 were mainly due to the flavonoid compounds, especially compounds *14, 16, 17, 18, 20, 21, 22, 23* were identified as flavonols and compounds *7* and *12* were identified as flava 3-ols (see Table 4). In vineyard 2, the differences were mainly due to the non-flavonoid compounds (compounds *2-6, 8, 9*), and especially to the hydroxycinnamic acids. Despite of the differences showed in diverse phenolic families, the same trend becomes evident, with higher content of hydroxycinnamic acids (significant differences in vineyard 2) and lower content of flavonols (significant differences in vineyard 1), especially for kaempferol derivatives (peak numbers *16, 17, 18, 19* and *20*), in S than in A leaves. In summary, some irregular changes on the phenolic composition of Tempranillo grapevine leaves were induced in response to Esca – GLSD. The finding of higher amounts of hidroxycinamic acids in Esca – GLSD symptomatic leaves is in agreement with previous reports of differential phenolic production in affected leaves of cv. Alvarinho (Lima et al., 2017). In contrast, a decrease in the content of some identified flavonols was also stated here. The studied vineyards differed in climatic conditions and availability of water. Curiously, minor changes in the phenolic profile of S and A leaves from vineyard 3 were obtained. At the time of leaf sampling (2016), vineyard 3 suffered from a severe restriction of water (lower than -0.4 MPa, see section 3.2 and Table 3) and significant differences in the A_N,

gs and E activity between the two groups of vines were evident (Table 3). Otherwise, vines with no drastic alterations on the physiological parameters (see data of Table 3 section 2.3 for vineyard 1 and 2 in 2016) manifested significant changes in the phenolic composition of S and A leaves. Differential phenolic production is related to biotic and abiotic stress (Lima et al., 2017). Our results suggested that Esca might cause changes in the different phenolic families. However, these might be not strictly related to fungal disease but predisposed by the environmental and physiological conditions. Further metabolomics studies could help in this context.

3.5. Gene expression

Changes in expression of photosynthesis, stress and defense related-genes were evaluated (Table 5). Results represent the relative expression of genes in leaves from S plants compared to leaves from A plants. Genes were considered to be significantly up- or downregulated when changes of their expression were > 2 x or < 0.5x, respectively. The repression of photosynthesis related genes has been observed in the apoplectic and leaf stripe forms of Esca disease plants of cv. Chardonnay (Letousey et al., 2010; Magnin-Robert et al., 2011). By contrast, in cv. Tempranillo, no changes in the expression of *RbcL* and *SBP* were observed in S vines of the three evaluated vineyards. Concerning the genes related to water stress a slight down-regulation (0.45) of the plasma membrane intrinsic aquaporin (*PIP 2.2*) gene was found only in the S vines of vineyard 2. Down regulation of aquaporins resulted in a perturbation to drought stress adaptation (Vandeleur et al., 2009). Similar trends were obtained in vines of cv. Aragonez (synonym of Tempranillo) artificially inoculated with Botryosphaeriaceae (*N. parvum* and *D. seriata*) (Reis et al., 2016) and plants of cv. Ugni Blanc affected by GTDs (Valtaud et al., 2011). In vineyard 1, the expression of *SOD*, encoding a superoxide dismutase and *GST5* (glutathione-*S*-transferase) was up-regulated (2.14 and

9.79, respectively) in vines with GLSD symptoms. These genes encode enzymes involved in detoxification processes and are known to prevent oxidative stress by catalyzing the conjugation of reduced glutathione (Magnin-Robert et al., 2011). A weak repression of *SOD* was observed in leaves of plants inoculated with *N. parvum* (Reis et al., 2016) and also in vineyard plants affected by Esca proper (Magnin-Robert et al., 2011), suggesting a possible lack of oxidative stress control which could be lethal for plants (Letousey et al., 2010). Interestingly, the genes *Chit 1b* (values from 3.81 to 4.83), *STS* (values from 2.57 to 6.26), and *PR6* (values from 33.12 to 55.58), all of them related with the defense pathway, were weakly expressed in GLSD vines regardless of the vineyard (Table 5). These results are consistent with various studies describing also an up-regulation of genes encoding chitinases (such as the case of *Chit 1b* used in this work), stilbenic phytoalexins (*STS* gene) and pathogenesis related proteins (namely PR such as *PR6* used in this work) in leaves of field-grown grapevines affected by GTDs (Letousey et al., 2010; Magnin-Robert et al., 2011) and artificially inoculated with *P. chlamydospora* (Lambert et al., 2013) and Botryosphaeriaceae (Reis et al., 2016). Furthermore, in symptomatic vines leaves of a Trebbiano d'Abruzzo vineyard the levels of phytoalexins at early appearance of symptoms were much lower compared with leaves with increased severity of symptoms (Calzarano et al., 2017). Altogether, our data suggest that these genes could be good markers of Esca stress response in cv. Tempranillo. This knowledge could be applied to asses rapid and non-destructive diagnostic methods and searching for resistance to GTD among Tempranillo clones.

In summary, this research reveals new insights on the physiological and genetical responses of cv. Tempranillo to Esca complex pathogens under different field conditions. In general, leaves from S vines showed a decrease of net photosynthesis

(A_N) more linked with a lower content of photosynthetic pigments than with the modulation of genes *RbcL* and *SBP*. More similar results were found in vineyards 1 and 2 with annual mean temperatures <15 ºC, no water restriction and highest GLSD incidence (6 % to 30 %). By one hand, changes on the phenolic profile of hydroxycinnamic acids and flavonoid compounds were found when comparing S and A grapevines. On the other hand, S vines overexpress defense-related genes (*Chit 1b*; *CHV5*, *STS*, *GST5* and *PR6*), encoding chitinases, stilbenic phytoalexins and PR proteins. The disturbance of physiological activity due to Esca disease was found to be amplified under water restriction conditions determined in vineyard 3 (annual mean temperature 15.79 ºC and 1% to 3% of GLSD incidence) while the changes on the phenolic compositions were modulated. As vineyard 3 is the one showing the lowest number of external symptoms, age of vines may explain in part this finding.

4. CONCLUSION

To conclude, valuable information on foliage alteration produced by Esca disease affecting Tempranillo has been generated at a physiological, chemical, and molecular level. Net leaf photosynthesis (A_N), photosynthetic pigments, flavonols and hydroxicinamic acids content as well as the expression of genes, namely *Chit 1b*, *STS*, and *PR6,* are proposed as potential physiological markers for future studies of Esca - GLSD tolerance in cv. Tempranillo. The changes of these markers over the growing season before the appearance of foliar symptoms and during the development of symptoms remain to be clarified but may help to develop further tools for a rapid and non-destructive diagnosis.

538 **Abbreviations Used**

539 A, asymptomatic, S, symptomatic, qRT-PCR, quantitative reverse transcription
540 polymerase chain reaction; GTDs, grapevine trunk diseases; GLSD, grapevine leaf
541 stripe disease; ITS, internal transcribed spacer; HPLC-DAD-MS, high performance
542 liquid chromatography coupled with diode array detection and mass spectrometry; A_N,
543 net leaf photosynthesis, gs, stomatal conductance; E, transpiration; Ψ_{leaf}, leaf water
544 potential; WUEi, intrinsic water use efficiency; Ci, internal leaf CO_2 concentration.

545

546 **Author's contributions**

547 LM conceived the study, she participated in its design and coordination. LM also
548 carried out the isolation and identification of pathogens, partial RT-PCR, statistical
549 analysis and drafted the manuscript. FF contributed to improve the study design and the
550 final manuscript. FJC and RR collected samples in the field and performed the
551 physiological measurements and its statistical analysis. AS and JV completed the RT-
552 PCR and the gene expression study. RFG performed the HPLC-DAD-MS analysis and
553 the compounds identification, and contributed to photosynthetic pigments determination
554 and the redaction of the manuscript.

555 **Acknowledgement**

556 The authors would like to acknowledge the financial support of the RETMAVID15
557 Project (Ref. RTC-2015-3492-2). The authors also thank Bodegas RODA S.A. (Haro,
558 La Rioja, Spain) project VINySOST, Programa Estratégico de Consorcios de
559 Investigación Empresarial Nacional 2014 (CIEN), for supplying the experimental
560 vineyards. Dra. L. Martín was supported by PTQ-13-06472 (Ministry of Economy and
561 Competitiveness). A part of this research was conducted during the STSM of Laura

562 Martin in the COST Action FA1303. COST Action is supported by the EU RTD
563 Framework program and ESF provides the COST Office through an EC contract.

564

565 **References**

566 Bertamini, M., Nedunchezhian, N., Tomasi, F., Grando, M.., 2002. Phytoplasma
567 [Stolbur-subgroup (Bois Noir-BN)] infection inhibits photosynthetic pigments,
568 ribulose-1,5-bisphosphate carboxylase and photosynthetic activities in field grown
569 grapevine (*Vitis vinifera* L. cv. Chardonnay) leaves. Physiol. Mol. Plant Pathol. 61,
570 357–366. https://doi.org/10.1006/pmpp.2003.0449

571 Bertsch, C., Ramírez-Suero, M., Magnin-Robert, M., Larignon, P., Chong, J., Abou-
572 Mansour, E., Spagnolo, A., Clément, C., Fontaine, F., 2013. Grapevine trunk
573 diseases: complex and still poorly understood. Plant Pathol. 62, 243–265.
574 https://doi.org/10.1111/j.1365-3059.2012.02674.x

575 Bruez, E., Vallance, J., Gerbore, J., Lecomte, P., Da Costa, J.P., Guerin-Dubrana, L.,
576 Rey, P., 2014. Analyses of the temporal dynamics of fungal communities
577 colonizing the healthy wood tissues of esca leaf-symptomatic and asymptomatic
578 vines. PLoS One 9. https://doi.org/10.1371/journal.pone.0095928

579 Bruno, G., Sparapano, L., 2006. Effects of three esca-associated fungi on *Vitis vinifera*
580 L.: III. Enzymes produced by the pathogens and their role in fungus-to-plant or in
581 fungus-to-fungus interactions. Physiol. Mol. Plant Pathol. 69, 182–194.
582 https://doi.org/10.1016/j.pmpp.2007.04.006

583 Calzarano, F., D'Agostino, V., Pepe, A., Osti, F., Della Pelle, F., De Rosso, M.,
584 Flamini, R., Di Marco, S., 2016. Patterns of phytoalexins in the grapevine leaf
585 stripe disease (esca complex) / grapevine pathosystem. Phytopathol. Mediterr. 55,
586 410–424. https://doi.org/10.14601/Phytopathol

587 Calzarano, F., Di Marco, S., D'Agostino, V., Schiff, S., Mugnai, L., 2014. Grapevine
588 leaf stripe disease symptoms (esca complex) are reduced by a nutrients and
589 seaweed mixture. Phytopathol. Mediterr. 53, 543–558.
590 https://doi.org/10.14601/Phytopathol
591 Calzarano, F., Osti, F., D'Agostino, V., Pepe, A., Della Pelle, F., De Roso, M., Flamini,
592 R., Di Marco, S., 2017a. Levels of phytoalexins in vine leaves with different
593 degrees of grapevine leaf stripe disease symtoms (Esca complex of diseases).
594 Phytopathol. Mediterr. 56, 494–501. https://doi.org/10.14601/Phytopathol
595 Calzarano, F., Osti, F., D'Agostino, V., Pepe, A., Di Marco, S., 2017b. Mixture of
596 calcium, magnesium and seaweed affects leaf phytoalexin contents and grape
597 ripening on vines with grapevine leaf stripe disease. Phytopathol. Mediterr. 56,
598 445–457. https://doi.org/10.14601/Phytopathol
599 Cartechini, A., Palliotti, A., 1995. Effect of shading on vine morphology and
600 productivity and leaf gas exchange characteristics in grapevines in the field. Am. J.
601 Enol. Vitic. 46, 227–234.
602 Chong, J., Le Henanff, G., Bertsch, C., Walter, B., 2008. Identification, expression
603 analysis and characterization of defense and signaling genes in *Vitis vinifera*. Plant
604 Physiol. Biochem. 46, 469–481. https://doi.org/10.1016/j.plaphy.2007.09.010
605 Crous, P., Gams, W., 2000. «*Phaeomoniella chlamydospora*» gen. et comb. nov., a
606 causal organism of Petri grapevine decline and esca. Phytopathol. Mediterr. 39,
607 112–118.
608 De la Fuente, M., Fontaine, F., Gramaje, D., Armengol, J., Smart, R., Nagy, Z.A.,
609 Borgo, M., Rego, C., Corio-Costet, M.F., 2016. Grapevine trunk diseases: A
610 review, OIV collective Expertise Document. ©OIV publications, 1st Edition: May
611 2016 (Paris, France). ISBN : 979-10-91799-60-7.

612 Di Gennaro, S.F., Battiston, E., Di Marco, S., Facini, O., Matese, A., Nocentini, M.,
613 Palliotti, A., Mugnai, L., 2016. Unmanned Aerial Vehicle (UAV)-based remote
614 sensing to monitor grapevine leaf stripe disease within a vineyard affected by esca
615 complex. Phytopathol. Mediterr. 55, 262–275.
616 https://doi.org/10.14601/Phytopathol
617 Escalona, J.M., Flexas, J., Medrano, H., 1999. Stomatal and non-stomatal limitations of
618 photosynthesis under water stress in field-grown grapevines. Aust. J. Plant Physiol.
619 26, 421–433. https://doi.org/10.1071/PP01119
620 Fischer, M., 2002. A new wood-decaying basidiomycete species associated with esca of
621 grapevine: *Fomitiporia mediterranea* (Hymenochaetales). Mycol. Prog. 1, 315–
622 324.
623 Fischer, M., González García, V., 2015. An annotated checklist of European
624 basidiomycetes related to white rot of grapevine (*Vitis vinifera*). Phytopathol.
625 Mediterr. 54, 281–298. https://doi.org/10.14601/Phytopathol
626 Fontaine, F., Pinto, C., Vallet, J., Clément, C., Gomes, A.C., Spagnolo, A., 2016. The
627 effects of grapevine trunk diseases (GTDs) on vine physiology. Eur. J. Plant
628 Pathol. 144, 707–721. https://doi.org/10.1007/s10658-015-0770-0
629 Glass, N.L., Donaldson, G.C., 1995. Development of primer sets designed for use with
630 the PCR to amplify conserved genes from filamentous ascomycetes. Appl.
631 Environ. Microbiol. 61, 1323-1330.
632 Gramaje, D., Mostert, L., Groenewald, J.Z., Crous, P.W., 2015. *Phaeoacremonium*:
633 From esca disease to phaeohyphomycosis. Fungal Biol. 119, 759–783.
634 https://doi.org/10.1016/j.funbio.2015.06.004
635 Gramaje, D., Urbez-Torres, J.R., Sosnowski, M.R., 2018. Managing grapevine trunk
636 diseases with respect to etiology and epidemiology: current strategies and future

637 prospects. Plant Dis. 102, 12–39. https://doi.org/10.1094/PDIS-04-17-0512-FE
638 Hasan, M.M., Bae, H., 2017. An overview of stress-induced resveratrol synthesis in
639 grapes: Perspectives for resveratrol-enriched grape products. Molecules 22.
640 https://doi.org/10.3390/molecules22020294
641 Hellemans, J., Mortier, G., De Paepe, A., Speleman, F., Vandesompele, J., 2007. qBase
642 relative quantification framework and software for management and automated
643 analysis of real-time quantitative PCR data. Genome Biol. 8, R19.
644 https://doi.org/10.1186/gb-2007-8-2-r19
645 Hidalgo, L., Hidalgo, J., 2011. Tratado de viticultura. Cap. XXIX El riego de la vid., 4ª
646 Edición. Ed. Mundi-Prensa S.A., Madrid-México. ISBN: 978-84-8476-424-3
647 Kimura, M., 1980. A simple method for estimating evolutionary rate of base
648 substitutions through comparative studies of nucleotide sequences. J. Mol. Evol.
649 16, 111–120.
650 Kortekamp, A., 2006. Expression analysis of defence-related genes in grapevine leaves
651 after inoculation with a host and a non-host pathogen. Plant Physiol. Biochem. 44,
652 58–67. https://doi.org/10.1016/j.plaphy.2006.01.008
653 Kottek, M., Grieser, J., Beck, C., Rudolf, B., Rubel, F., 2006. World map of the
654 Köppen-Geiger climate classification updated. Meteorol. Zeitschrift 15, 259–263.
655 https://doi.org/10.1127/0941-2948/2006/0130
656 Lambert, C., Khiook, I.L.K., Lucas, S., Telef-Micouleau, N., Merillon, J.-M., Cluzet, S.,
657 2013. A faster and a stronger defense response: One of the key elements in
658 grapevine explaining its lower level of susceptibility to esca? Phytopathology 103,
659 1028–1034. https://doi.org/10.1094/PHYTO-11-12-0305-R
660 Larignon, P., Dubos, B., 1997. Fungi associated with esca disease in grapevine. Eur. J.
661 Plant Pathol. 103, 147–157. https://doi.org/10.1023/A:1008638409410

662 Letousey, P., Baillieul, F., Perrot, G., Rabenoelina, F., Boulay, M., Vaillant-Gaveau, N.,
663 Clément, C., Fontaine, F., 2010. Early events prior to visual symptoms in the
664 apoplectic form of grapevine esca disease. Phytopathology 100, 424–431.
665 https://doi.org/10.1094/PHYTO-100-5-0424
666 Lima, M.R.M., Felgueiras, M.L., Cunha, A., Chicau, G., Ferreres, F., Dias, A.C.P.,
667 2017. Differential phenolic production in leaves of Vitis vinifera cv. Alvarinho
668 affected with esca disease. Plant Physiol. Biochem. 112, 45–52.
669 https://doi.org/10.1016/j.plaphy.2016.12.020
670 Luque, J., Martos, S., Aroca, A., Raposo, R., Garcia-Figueres, F., 2009. Symptoms and
671 fungi associated with declining mature grapevine plants in northeast Spain. J. Plant
672 Pathol. 91, 381–390.
673 Magnin-Robert, M., Adrian, M., Trouvelot, S., Spagnolo, A., Jacquens, L., Letousey, P.,
674 Rabenoelina, F., Harir, M., Roullier-Gall, C., Clément, C., Schmitt-Kopplin, P.,
675 Vallat, A., Abou-Mansour, E., Fontaine, F., 2017. Alterations in grapevine leaf
676 metabolism occur prior to esca apoplexy appearance. Mol. Plant-Microbe Interact.
677 30, 946–959. https://doi.org/10.1094/MPMI-02-17-0036-R
678 Magnin-Robert, M., Letousey, P., Spagnolo, A., Rabenoelina, F., Jacquens, L., Mercier,
679 L., Clement, C., Fontaine, F., 2011. Leaf stripe form of esca induces alteration of
680 photosynthesis and defence reactions in presymptomatic leaves. Funct. Plant Biol.
681 38, 856–866. https://doi.org/10.1071/FP11083
682 Martín, L., Castaño, F.J., Durante, G., Chatillon, C., Luque, J., 2015. A new molecular
683 diagnostic tool for detection of Botryosphaeriaceae species. Phytopathol. Mediterr.
684 54, 425.
685 Martín, L., Martín, M.T., 2013. Multi-gene sequence analysis and phenotypic diversity
686 of *Phaeoacremonium* species isolated from grapevines in Spain. Eur. J. Plant

687 Pathol. 137, 343–361. https://doi.org/10.1007/s10658-013-0247-y
688 Martín, M.T., Cuesta, M.J., Martín, L., 2014. Development of SCAR primers for PCR
689 assay to detect *Diplodia seriata*. Int. Sch. Res. Not. Article ID 824106.
690 https://doi.org/doi:10.1155/2014/824106
691 Martin, N., Vesentini, D., Rego, C., Monteiro, S., Oliveira, H., Ferreira, R.B., 2009.
692 *Phaeomoniella chlamydospora* infection induces changes in phenolic compounds
693 content in *Vitis vinifera*. Phytopathol. Mediterr. 48, 101–116.
694 Mondello, V., Songy, A., Bttiston, E., Pinto, C., Coppin, C., Trotel-Aziz, P., Clément,
695 C., Mugnai, L., Fontaine, F., 2018. Grapevine trunk diseases: a review of fifteen
696 years of trials for their control with chemicals and biocontrol agents. Plant Dis.
697 102, 1189–1217.
698 Moriondo, M., 2005. The effect of downy and powdery mildew on grapevine (*Vitis*
699 *vinifera* L .) leaf gas exchange. Vitis 357, 350–357. https://doi.org/10.1111/j.1439-
700 0434.2005.00984.x
701 Mugnai, L., Graniti, A., Surico, G., 1999. Esca (black measles) and brown wood-
702 streaking : two old and elusive diseases of grapevines. Plant Dis. 83, 404–418.
703 O'Donnell, K., Cigelinik, E., 1997. Two different intragenomic rDNA ITS2 types
704 within a monophyletic lineage of the fungus *Fusarium* are nonorthologous. Mol.
705 Phylogenet. Evol. 7, 103–116.
706 Petit, A.N., Vaillant, N., Boulay, M., Clément, C., Fontaine, F., 2006. Alteration of
707 photosynthesis in grapevines affected by esca. Phytopathology 96, 1060–1066.
708 https://doi.org/10.1094/PHYTO-96-1060
709 Reis, P., Magnin-Robert, M., Nascimento, T., Spagnolo, A., Abou-Mansour, E.,
710 Fioretti, C., Clément, C., Rego, C., Fontaine, F., 2016. Reproducing
711 Botryosphaeria dieback foliar symptoms in a simple model system. Plant Dis. 100,

712 1071–1079. https://doi.org/10.1094/PDIS-10-15-1194-RE
713 Surico, G., 2009. Towards a redefinition of the diseases within the esca complex of
714 grapevine. Phytopathol. Mediterr. 48, 5–10.
715 Tamura, K., Stecher, G., Peterson, D., Filipski, A., Kumar, S., 2013. MEGA6:
716 Molecular evolutionary genetics analysis version 6.0. Mol. Biol. Evol. 30, 2725–
717 2729. https://doi.org/10.1093/molbev/mst197
718 Tomás, M., Medrano, H., Escalona, J.M., Martorell, S., Pou, A., Ribas-Carbo, M.,
719 Flexas, J., 2014. Variability of water use efficiency in grapevines. Environ. Exp.
720 Bot. 103, 148–157. https://doi.org/10.1016/j.envexpbot.2013.09.003
721 Valtaud, C., Thibault, F., Larignon, P., Bertsch, C., Fleurat-Lessard, P., Bourbouloux,
722 A., 2011. Systemic damage in leaf metabolism caused by esca infection in
723 grapevines. Aust. J. Grape Wine Res. 17, 101–110. https://doi.org/10.1111/j.1755-
724 0238.2010.00122.x
725 Vandeleur, R.K., Mayo, G., Shelden, M.C., Gilliham, M., Kaiser, B.N., Tyerman, S.D.,
726 2009. The role of plasma membrane intrinsic protein aquaporins in water transport
727 through roots: diurnal and drought stress responses reveal different strategies
728 between isohydric and anisohydric cultivars of grapevine. Plant Physiol. 149, 445–
729 460.
730 White, T.J., Bruns, T.D., Lee, S., Taylor, J., 1990. Amplification and direct sequencing
731 of fungal ribosomal RNA genes for phylogenetics., in: PCR Protocols: A Guide to
732 Methods and Applications. pp. 315–322. Academic Press, San Diego, California.
733

734 **Figure captions**

735 **Figure 1**. a) Geographical location of the three studied vineyards in Spain. b)
736 Representative sample of the studied symptomatic (at left) and asymptomatic leaves (at
737 right).

738

739 **Figure 2**. Phylogenetic tree based on the alignment of the ITS sequences of fungi
740 isolated from S vines in this study. The optimal tree with the sum of branch length =
741 1.22471915 is shown. The percentage of replicate trees in which the associated taxa
742 clustered together in the bootstrap test (1,000 replicates) is shown next to the branches.
743 The tree is drawn to scale, with branch lengths in the same units as those of the
744 evolutionary distances used to infer the phylogenetic tree. ■ Isolates identified in this
745 study from S vines of vineyard 1; ♦ Isolates identified in this study from S vines of
746 vineyard 2; ● Isolates identified in this study from S vines of vineyard 3.

747

748 **Figure 3**. The content of chlorophylls (a) and carotenoids (b) (dry weight) in A
749 (Asymptomatic) and S (Symptomatic) Tempranillo leaves. *Significant differences at p
750 < 0.05 between A and S samples (n=12) collected in 2016 when first GLSD symptoms
751 appeared. Leaf samples were taken at beginning of berry ripening at the same date of
752 physiological determinations.

753

754 **Figure 4.** (a) HPLC chromatogram of leaf extracts and identified phenolic compounds
755 from grapevine leaves registered at 306 nm. Number of the identified compounds refers
756 to Table 4. (b) Differences on the phenolic compounds of symptomatic (S) and
757 asympotomatic (A) leaf samples from the three studied vineyards. *Significant
758 differences at p < 0.05 between A and S samples (n=8) collected in 2016 when first

759 GLSD symptoms appeared. Leaf samples were taken at beginning of berry ripening at
760 the same date of physiological determinations.

761

Table 1: Monthly mean temperatures (T_m); Monthly mean of maximum temperatures (T_{MAX}); Monthly mean of minimum temperatures (T_{min}); monthly accumulated precipitation (P_m); annual accumulated precipitation (P_a) in the studied vineyards.

Vineyard 1 – Rioja (North Spain)					
Year	Month	T_m (ºC)	T_{MAX} (ºC)	T_{min} (ºC)	P_m (mm)
2013	Jan	6.4	10.5	2.6	58.6
	Feb	5.2	8.7	2.3	81.8
	Mar	8.3	12.9	4.6	102.8
	Apr	10.3	15.5	5.3	54.8
	May	10.8	16.0	6.6	60.6
	Jun	15.6	21.7	10.2	70.2
	Jul	22.3	30.8	14.8	35.0
	Aug	20.3	27.8	14.3	3.8
	Sep	17.6	25.5	11.4	23.2
	Oct	14.4	21.1	9.3	27.6
	Nov	8.4	11.7	5.6	90.8
	Dec	4.3	8.5	1.1	29.2
	2013	11.99 ± 5.98	17.56 ± 7.66	7.34 ± 4.62	P_a = 638.40
2014	Jan	6.8	10.3	3.7	29.6
	Feb	6.5	11.3	1.9	32.3
	Mar	8.8	14.6	3.0	46.0
	Apr	13.3	19.9	7.9	22.4
	May	13.6	19.8	8.1	20.8
	Jun	18.6	26.7	11.7	42.0
	Jul	19.7	27.4	13.7	27.2
	Aug	20.2	28.6	13.9	0.8
	Sep	19.2	27.5	12.7	77.2
	Oct	15.2	22.9	9.6	23.6
	Nov	10.1	13.8	6.7	130.8
	Dec	5.9	9.2	3.0	76.0
	2014	13.16 ± 5.47	19.33 ± 7.31	7.99 ± 4.40	P_a = 528.70
2015	Jan	4.2	8.7	0.5	48.7
	Feb	3.8	7.3	0.9	76.0
	Mar	8.7	14.2	4.1	59.4
	Apr	12.6	18.4	7.1	19.2
	May	15.5	21.9	9.9	1.6
	Jun	19.3	27.3	12.8	59.6
	Jul	22.6	31.8	15.8	15.2
	Aug	21.1	29.7	13.7	58.3
	Sep	16.1	23.6	10.3	19.9
	Oct	12.9	19.4	7.6	36.8
	Nov	9.3	14.4	5.4	27.0
	Dec	5.7	10.3	2.0	3.0
	2015	12.65 ± 6.46	18.92 ± 8.20	7.51 ± 5.12	P_a = 424.70
2016	Jan	7.0	10.5	3.7	34.8
	Feb	6.8	11.5	2.8	91.1
	Mar	7.1	11.8	2.9	88.6

	Apr	9.6	15.3	4.7	42.4
	May	14.5	20.9	8.9	24.8
	Jun	18.7	26.0	12.5	16.2
	Jul	21.2	28.7	15.4	16.2
	Aug	21.7	30.1	14.2	10.6
	Sep	19.2	27.1	12.7	41.8
	Oct	13.7	21.1	8.1	12.8
	Nov	8.5	12.9	4.6	111.0
	Dec	5.9	8.8	3.3	11.4
	2016	12.83 ± 6.09	18.73 ± 7.83	7.82 ± 4.79	P_a = 501.70
Mean (2013-2016) ± SD		**12.66 ± 0.49**	**18.64 ± 0.76**	**7.66 ± 0.29**	**523.38 ± 88.44**
Vineyard 2 - Catalonia (North East Spain)					
2013	Jan	4.6	17.3	-4.1	34.2
	Feb	6	17.1	-5.1	14.7
	Mar	10.1	21.2	-1.4	58.2
	Apr	12.3	27.4	-0.2	74.3
	May	13.9	25.9	2.9	14.6
	Jun	19.3	32.5	6.9	38.1
	Jul	24.5	34.5	15.1	38.4
	Aug	22.6	33.5	10.7	22.1
	Sep	19.3	31	6.7	7.2
	Oct	16.2	29.5	0.6	5.3
	Nov	8.7	24	-5.6	64.7
	Dec	3	13.7	-4.8	10.8
	2013	13.38 ± 7.14	25.63 ± 7.02	1.81 ± 6.77	P_a = 382.60
2014	Jan	6.7	18.7	-1.9	31.7
	Feb	7.2	18.6	-2.9	16.7
	Mar	10.2	23.4	0	12.8
	Apr	15	26	4.7	44.2
	May	16	28.7	2.8	22.7
	Jun	21.4	32.4	9.6	10.4
	Jul	22.4	34.6	9.8	6
	Aug	22.8	34.6	9.6	41.2
	Sep	20.8	32	8.1	118.6
	Oct	16.7	28.5	3.9	21.4
	Nov	11.3	20.8	-0.1	108.4
	Dec	5	16.1	-6.4	11.1
	2014	14.63 ± 6.46	26.20 ± 6.60	3.10 ± 5.47	P_a = 445.20
2015	Jan	3.6	14.5	-5.6	16
	Feb	5.2	18.8	-5	19.6
	Mar	10.8	22.2	-2.1	29.6
	Apr	13.9	26.3	1.9	8.6
	May	18.2	31.8	4.9	2
	Jun	22	36	11.6	40.9
	Jul	25.6	39.3	12.1	29.7
	Aug	23.2	37.6	10.2	19.1
	Sep	17.9	30.4	6	12.9

	Oct	14.4	25.5	0.4	9.3
	Nov	9.8	22.4	-5.5	64.5
	Dec	5.8	16	-4	4.7
	2015	14.20 ± 7.36	26.73 ± 8.37	2.08 ± 6.77	P_a = 256.90
2016	Jan	7	18	-5.6	14.4
	Feb	7.3	19.9	-4.7	72.4
	Mar	8.8	24	-1.5	28.9
	Apr	12.4	24.5	1.6	63.3
	May	15.7	27.7	1.2	40.7
	Jun	21	32.9	8.1	7.5
	Jul	24.1	37.2	9.8	1.6
	Aug	23.2	35.2	10.2	3.1
	Sep	20.6	36.6	5.9	5
	Oct	15.1	27.6	2.3	30
	Nov	8.6	18.5	-1.8	72
	Dec	4.4	16.7	-3	7.1
	2016	14.02 ± 6.93	26.57 ± 7.52	1.88 ± 5.52	P_a = 346.00
Mean (2013-2016) ± SD		**14.36 ± 0.29**	**26.28 ± 0.49**	**2.22 ± 0.60**	**357.68 ± 76.68**
Vineyard 3 – Castilla La Mancha (Centre Spain)					
2013	Jan	6.29	11.52	1.60	14.40
	Feb	6.59	12.79	0.91	16.70
	Mar	9.67	14.31	5.33	82.10
	Apr	12.65	19.05	6.01	23.40
	May	15.17	22.98	6.94	20.00
	Jun	21.68	30.22	12.57	7.70
	Jul	26.69	36.15	16.92	2.50
	Aug	25.95	35.73	16.57	13.40
	Sep	22.03	30.49	14.05	20.50
	Oct	15.51	22.39	10.03	70.50
	Nov	8.15	14.95	2.22	12.60
	Dec	4.51	11.91	-1.02	67.30
	2013	14.57 ± 7.90	21.87 ± 9.26	7.68 ± 6.26	P_a = 351.10
2014	Jan	9.30	12.90	1.10	69.90
	Feb	11.10	14.80	7.40	91.60
	Mar	14.10	18.70	9.50	14.20
	Apr	15.18	22.50	7.86	29.30
	May	18.24	26.30	9.53	10.60
	Jun	22.40	30.16	13.57	0.20
	Jul	24.54	32.81	15.60	0.10
	Aug	24.94	33.29	15.63	0.00
	Sep	20.63	28.20	14.27	0.30
	Oct	17.04	24.44	11.12	81.50
	Nov	11.45	15.92	7.44	70.50
	Dec	5.42	12.29	0.65	13.20
	2014	16.19 ± 6.23	22.69 ± 7.66	9.47 ± 5.01	P_a = 381.40
2015	Jan	4.13	12.69	-1.79	16.80
	Feb	6.78	12.62	0.80	12.10

	Mar	10.47	18.40	3.25	35.70
	Apr	14.21	21.37	7.45	40.20
	May	19.37	28.36	11.61	4.57
	Jun	24.04	32.43	15.04	19.81
	Jul	28.18	36.25	18.99	0.25
	Aug	24.15	34.21	14.49	39.11
	Sep	18.67	27.94	10.20	15.75
	Oct	15.38	21.57	10.38	65.79
	Nov	10.37	18.13	4.84	29.95
	Dec	7.20	14.26	2.07	7.86
	2015	15.25 ± 7.75	23.19 ± 8.44	8.11 ± 6.41	P_a = 287.89
2016	Jan	8.32	12.60	4.29	27.73
	Feb	8.61	13.79	3.84	27.50
	Mar	9.00	15.58	3.04	26.40
	Apr	12.46	18.20	7.02	85.60
	May	16.03	22.23	10.04	48.25
	Jun	23.04	31.47	13.22	0.00
	Jul	27.66	36.63	18.31	3.56
	Aug	27.12	35.96	18.63	1.52
	Sep	22.21	31.52	12.74	4.06
	Oct	16.22	23.64	9.97	33.25
	Nov	9.47	14.76	4.91	78.31
	Dec	6.829	12.645	3.08	1.95
	2016	15.58 ± 7.67	22.42 ± 9.25	9.09 ± 5.67	P_a = 338.13
2017	Jan	4.89	11.42	-0.82	20.56
	Feb	9.05	14.14	4.41	22.49
	Mar	10.85	18.55	4.57	16.00
	Apr	15.54	23.83	7.51	9.39
	May	19.60	27.33	11.44	28.95
	Jun	25.79	34.22	16.94	8.89
	Jul	26.54	35.32	16.61	26.44
	Aug	27.01	36.41	16.75	32.00
	Sep	21.07	30.15	12.21	0.00
	Oct	17.30	26.88	9.22	11.80
	Nov	8.52	17.21	1.78	26.85
	Dec	5.91	12.40	0.84	35.31
	2017	16.01 ± 8.12	23.99 ± 9.09	8.46 ± 6.41	P_a = 238.68
Mean (2013 – 2017) ± SD		**15.52 ± 0.65**	**22.83 ± 0.80**	**8.56 ± 0.732**	**319.44 ± 56.37**

Table 2. Primers of genes analyzed by real-time reverse-transcription polymerase chain reaction.

Genes	Category	Primer sequences	Genbank or TC TIGR accession number
EF1-α (elongation factor 1-α)	Constitutive gene	5'-GAACTGGGTGCTTGATAGGC-3' 5'-AACCAAAATATCCGGAGTAAAAGA-3'	GU585871
SRP60 (60S ribosomal protein L18)	Constitutive gene	5'- ATCTACCTCAAGCTCCTAGTC-3' 5'-CAATCTTGTCCTCCTTTCCT-3'	XM_002270599
RbcL (large subunit of Rubisco)	Photosynthesis related gene	5'-AATTTTTCCTCCACGGCGATA-3' 5'-ATCTGCGCCCGCCTTTATA-3'	TC57584
SBP (sedoheptulose-7-biphosphatase, Calvin Cycle)	Photosynthesis related gene	5'-TGCCAACCAGCTCCTATTTGA-3' 5'-TCAACTGGGCCTCCCATGT-3'	XM_002263013
PIP2.2 (plasma membrane intrinsic aquaporin)	Water stress related gene	5'-GGTTCAGTCTCCATTGCACATG-3' 5'-TTGGCAGCACAGCAGATGTAT-3'	XM_002271336
EpoxHF (epoxide hydrolase)	Detoxification process gene	5'-TGCTCGTCTTGGCACTGAGA-3' 5'-TGAGCGCACCACTGTACCAT-3'	XM_003632333
SOD (superoxide dismutase)	Detoxification process gene	5'- GTGGACCTAATGCAGTGATTGGA-3' 5'- TGCCAGTGGTAAGGCTAAGTTCA-3'	AF056622
GST5 (Glutation-S-Transferase 5)	Stress tolerance	5'-GCAGAAGCTGCCAGTGAAATT-3' 5'-GGCAAGCCATGAAAGTGACA-3'	XM_002277883
Chit 1b (class I basic chitinase)	Defense related gene	5'-ATGCTGCAGCAAGTTTGGTT-3' 5'-CATCCTCCTGTGATGACATT-3'	Z54234
CHV5 (class V chitinase)	Defense related gene	5'-CTACAACTATGGCGCTGCTG-3' 5'-CCAAAACCATAATGCGGTCT-3'	AF532966
STS (stilbene synthase)	Defense related gene	5'- AGGAAGCAGCATTGAAGGCTC-3' 5'- TGCACCAGGCATTTCTACACC-3'	X76892
PR6 (serine proteinase inhibitor)	Pathogenesis related proteins	5'- AGGGAACAATCGTTACCCAAG-3' 5'- CCGATGGTAGGGACACTGAT-3'	AY156047

Table 3: Leaf water potential (Ψ_{leaf}) and its temperature, net leaf photosynthesis (A_N), stomatal conductance (gs), transpiration (E), internal CO_2 concentration and intrinsic water use efficiency (WUEi) in *Asymptomatic* (A) and *Symptomatic* (S) Esca Tempranillo vines. *Significant differences at $p < 0.05$ between A and S samples (n=8). Date of sampling when first GLSD symptoms appeared at beginning of berry ripening.

Year 1	Vineyard 1		Vineyard 2		Vineyard 3	
Date	7/7/2015		19/6/2015		3/8/2016	
	A	S	A	S	A	S
Ψ_{leaf} (MPa)	-0.81 ± 0.06	-0.91 ± 0.08	-0.82 ± 0.10	-0.87 ± 0.07	-1.45 ± 0.13	-1.48 ± 0.16
Leaf temperatura (ºC)	34.20 ± 0.47	35.08 ± 0.56	32.68 ± 0.38	32.38 ± 0.43	40.42 ± 0.53	40.37 ± 0.78
A_N (µmol/m^{2}s)	15.17 ± 0.83	14.67 ± 1.44	16.21 ± 0.79	15.58 ± 0.66	8.26 ± 0.45	4.83 ± 0.61 *
gs (mol/m^{2}s)	0.22 ± 0.02	0.27 ± 0.04	0.34 ± 0.04	0.29 ± 0.01	0.09 ± 0.01	0.04 ± 0.00 *
E (mmol/m^{2}s)	4.75 ± 0.42	5.55 ± 0.26	5.33 ± 0.18	4.95 ± 0.20	3.85 ± 0.22	1.97 ± 0.17 *
Ci (µmol/m^{2}s	206.50 ± 2.90	227.30 ± 11.56	237.00 ± 9.00	234.25 ± 4.89	160.70 ± 7.69	126.00 ± 9.92 *
WUEi (A_N/gs)	71.29 ± 3.34	56.13 ± 6.02	48.80 ± 4.65	54.21 ± 0.76	99.51 ± 5.06	126.40 ± 7.78 *

Year 2	Vineyard 1		Vineyard 2		Vineyard 3	
Date	19/7/2016		12/7/2016		26/7/2017	
	A	S	A	S	A	S
Ψ_{leaf} (MPa)	-0.87 ± 0.10	-0.72 ± 0.09	-0.81 ± 0.09	-0.90 ± 0.13	-1.12 ± 0.13	-1.27 ± 0.10
Leaf temperatura (ºC)	35.46 ± 0.32	35.83 ± 0.25	35.85 ± 0.42	36.67 ± 0.62	36.38 ± 0.83	36.24 ± 0.56
A_N (µmol/m^{2}s)	12.91 ± 1.05	12.27 ± 1.87	13.76 ± 0.53	10.22 ± 1.72	6.98 ± 1.62	5.80 ± 0.57
gs (mol/m^{2}s)	0.18 ± 0.02	0.18 ± 0.04	0.23 ± 0.02	0.17 ± 0.04	0.08 ± 0.02	0.06 ± 0.01
E (mmol/m^{2}s)	4.80 ± 0.26	4.79 ± 0.75	5.70 ± 0.64	4.22 ± 0.71	2.79 ± 0.49	2.35 ± 0.31
Ci (µmol/m^{2}s	200.60 ± 0.12	200.90 ± 0.14	222.10 ± 10.62	211.80 ± 7.54	183.60 ± 8.43	171.50 ± 4.74
WUEi (A_N/gs)	76.14 ± 3.34	73.25 ± 5.80	57.56 ± 6.57	69.20 ± 6.63	94.80 ± 7.59	107.10 ± 5.54

Table 4. Retention time (RT), wavelength of maximum absorption (λ), molecular ion M-H$^-$ (*m/z*), main fragments in MS^2 (*m/z*) and tentative identification of phenolic compounds from *Vitis vinifera* L. cv. Tempranillo grapevine leaf samples.

Peak number	RT	λ (nm)	[M -H]$^-$ (*m/z*)	MS^2 (*m/z*)	Tentative identification
1	3.8	270	329	195(35), 189(50), 165(15)	galloyl glucose
2	5.6	328	367	195 (25), 177(25), 153(10)	feruloylquinnic acid
3	6.4	292, 320	351	195(60), 189(40), 177(25), 153(10)	caffeoyquinnic acid
4	6.73	298	465	397(30), 381(100)	digalloyl glucose
5	7.55	286, 332	337	195(100), 177(80), 153(10)	coumaroylquinnic acid
6	8.59	298, 330	309	195(10), 177(100)	caffeoyltartaric acid
7	10.78	280	441	425(100)	catechin gallate
8	12.6	270, 306	477	383(40), 289(50), 195(100), 177(25), 153(10)	guaicol glucoside-derivative
9	13.41	268, 310	383	317(20), 298(60), 289(20), 195(100), 161(50)	guaiacol glucoside
10	16.4	244, 330	409	353(50), 269(50)	caffeoylquinnic acid derivative
11	18.4	280	577	425(40), 407(100), 289(50)	procyanidin dimer
12	21.8	282	619	407(100), 355(30), 285(15)	procyanidin dimer derivative
13	26.9	278	637	575(40), 559(30), 289	procyanidin dimer derivative
14	32	256, 356	463	301(100)	quercetin 3-*O*-glucoside
15	33.3	256, 357	477	301(100)	quercetin 3-*O*-glucuronide
16	37	264, 348	447	285(100)	Kaempferol 3-*O*- glucoside
17	37.9	266, 350	593	285(100)	Kaempferol 3-*O*-rutinoside
18	38.8	266, 350	447	285(100)	Kaempferol 3-*O*-hexoside
19	39	264, 350	461	285(100)	Kaempferol 3-*O*-glucuronide
20	39.9	258, 354	285		Kaempferol aglycone
21	41.8	264, 348	693	451(50), 353(40), 285(90)	Kaempferol derivative
22	43.9	266, 352	539	285(100)	Kaempferol derivative
23	44.8	260, 356	531	285(100)	Kaempferol derivative

Table 5. Relative expression of 10 selected genes. Results represent the relative expression of genes in leaves from S plants (n=4) versus leaves collected from A plants (n=4), in three vineyards of cv. Tempranillo. Genes were considered to be significantly up- or down-regulated when changes of their expression was > 2x or < 0.5x, respectively, compared to the control asymptomatic vines. The colour chart represents the level of up-regulation (red scale) and down-regulation (blue scale).

Genes	Category	Vineyard 1	Vineyard 2	Vineyard 3
RbcL	Photosynthesis related genes	0.60±0.09	1.45±0.11	0.95±0.06
SBP		0.72±0.03	1.28±0.14	0.83±0.04
PIP2.2	Water stress related gene	0.69±0.06	0.45±0.15	1.24±0.24
EpoxHF	Detoxification process and stress tolerance genes	1.18±0.06	1.62±0.11	0.92±0.10
SOD		2.14±0.35	0.87±0.17	1.56±0.06
GST5		9.79±1.40	1.12±0.12	1.26±0.20
Chit 1b	Pathogenesis and defense related genes	4.20±0.80	3.81±2.14	4.83±1.01
CHV5		21.99±6.58	3.60±3.09	1.13±0.37
STS		6.26±1.41	2.57±1.30	3.20±0.72
PR6		55.58±16.75	33.12±31.67	34.59±13.77

> 20 < 0.01

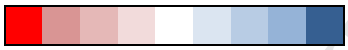

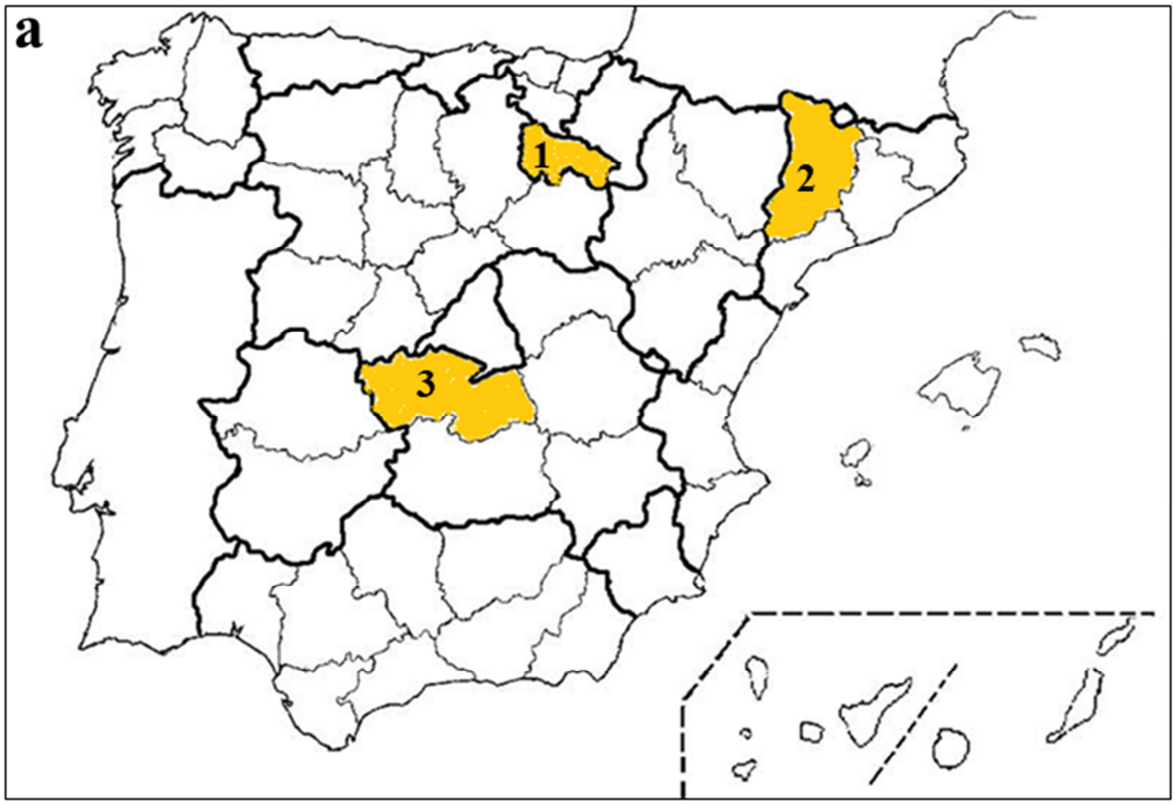
a
1
2
3


b

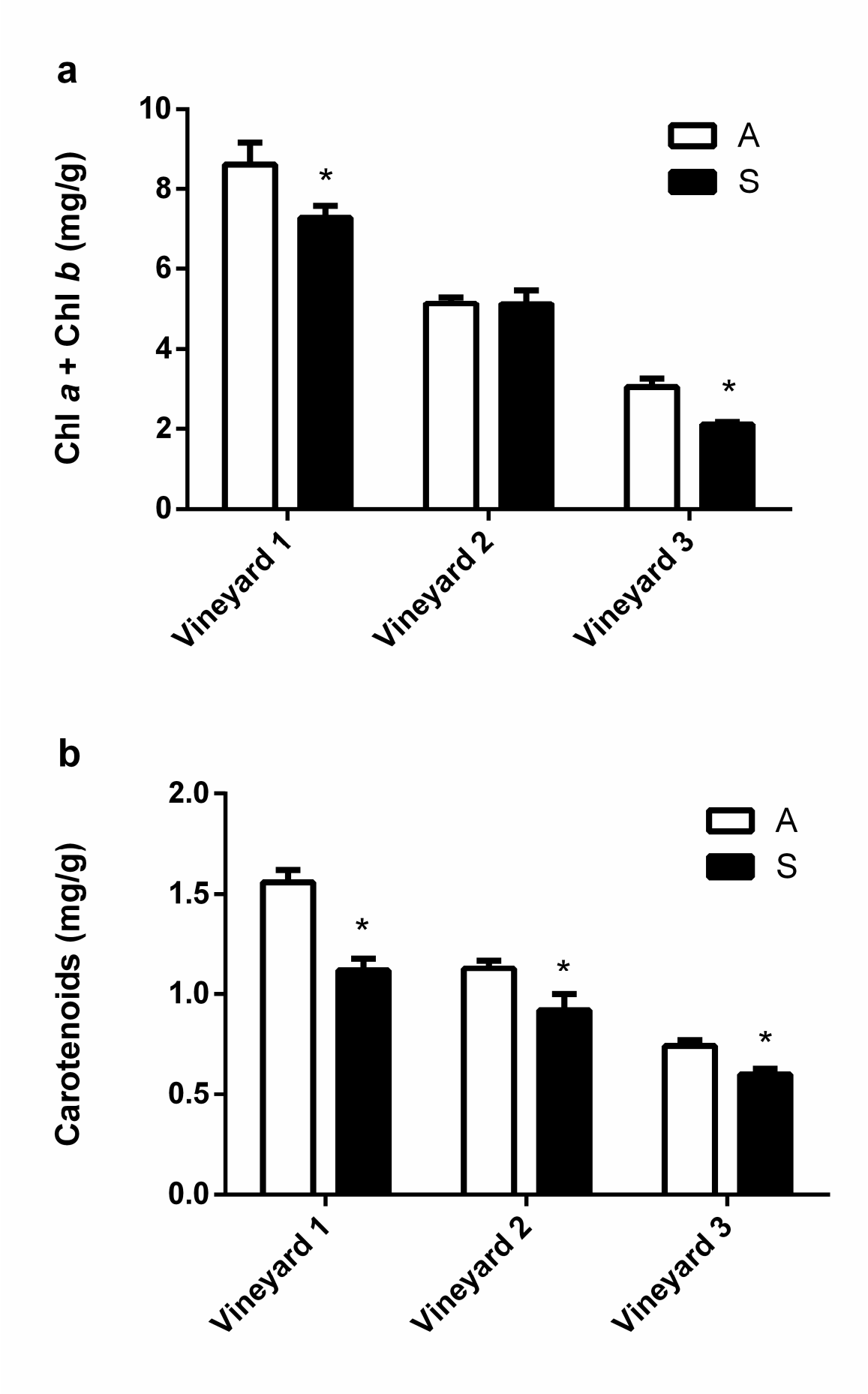
a
Chl a + Chl b (mg/g)
10
8
6
4
2
0
A
S
*
*
Vineyard 1
Vineyard 2
Vineyard 3
b
Carotenoids (mg/g)
2.0
1.5
1.0
0.5
0.0
A
S
*
*
*
Vineyard 1
Vineyard 2
Vineyard 3

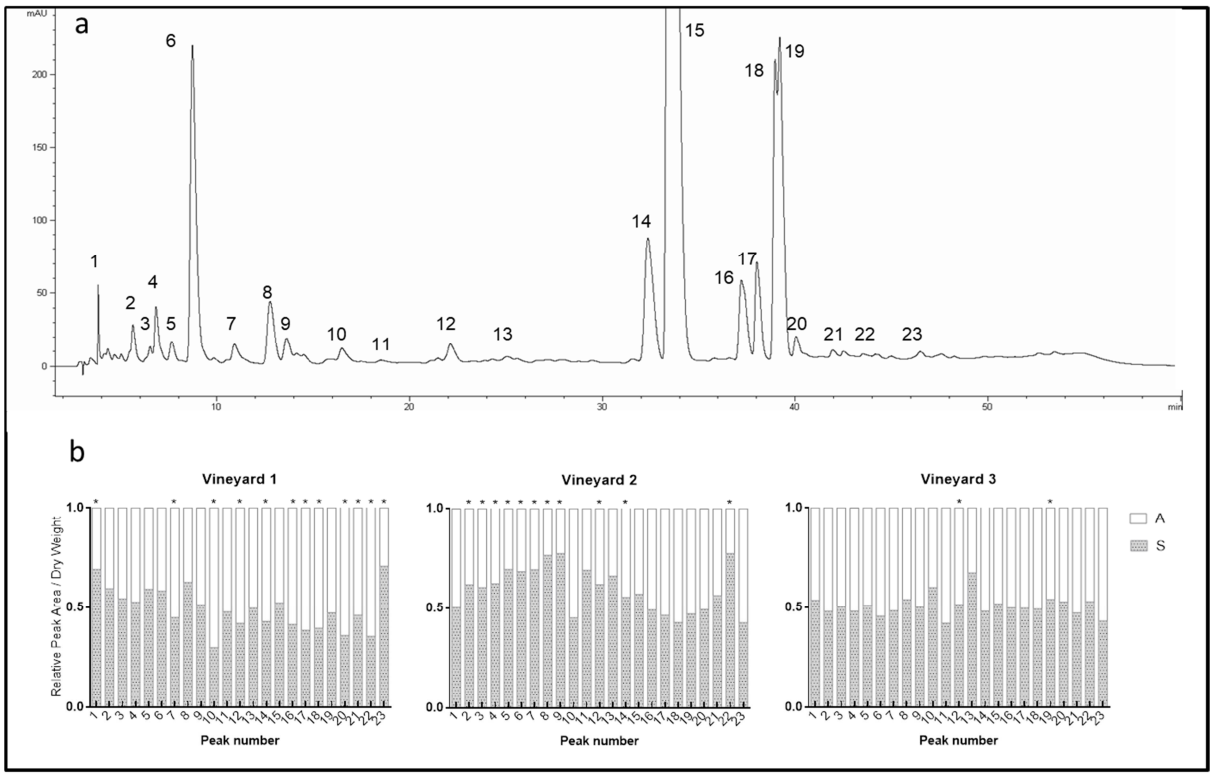

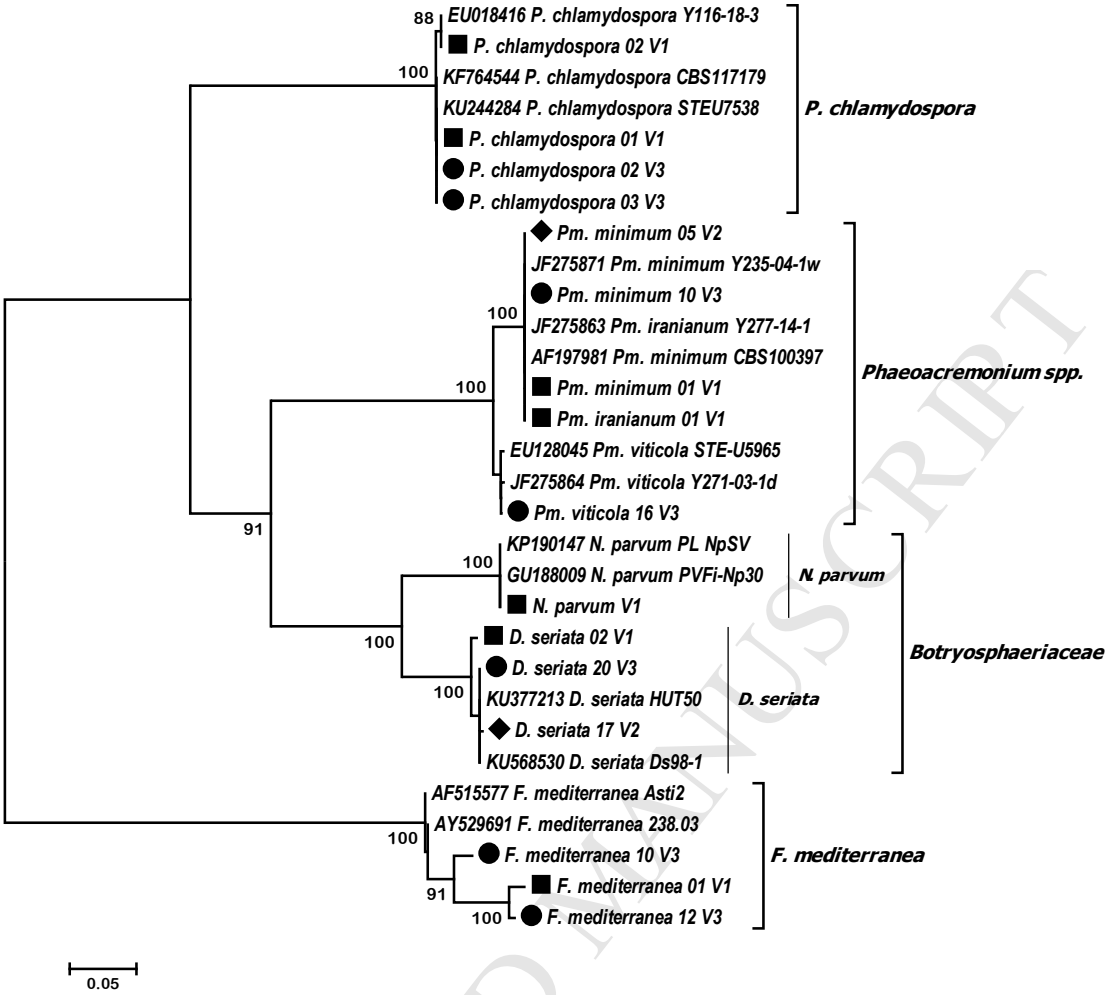

HIGHLIGHTS

- The photosynthetic pigments were reduced in Esca infected Tempranillo vines.
- Changes on the phenolic composition of Tempranillo leaves were induced in response to Esca infection.
- Esca Tempranillo vines overexpress defense-related genes, encoding chitinases, stilbenic phytoalexins and PR proteins.
- The disturbance of physiological activity due to Esca was intensified under drought condition.

CONTRIBUTION

LM conceived the study, she participated in its design and coordination. LM also carried out the isolation and identification of pathogens, partial RT-PCR, statistical analysis and drafted the manuscript. FF contributed to improve the study design and the final manuscript. FJC and RR collected samples in the field and performed the physiological measurements and its statistical analysis. AS and JV completed the RT-PCR and the gene expression study. RFG performed HPLC-DAD-MS analysis and the compounds identification, and contributed to photosynthetic pigments determination and the redaction of the manuscript.